Study of Radioactive Characteristics of Cement Pastes Blended with GGBFS

Ahmed S. Ouda[1,2(✉)]

[1] Concrete Chemistry and Building Materials, Housing & Building National Research Center, Dokki, Giza, Egypt
[2] Department of Chemistry, University College of Taimaa, Tabuk University, Tabuk, Kingdom of Saudi Arabia
Ahmed.Kamel56@yahoo.com

Abstract. This paper reports an experimental study carried out to investigate the effects of ground granulated blast- furnace slag (GGBFS) on radiation attenuation and mechanical properties of blended cements. Five cement mixtures were prepared with 0%, 10%, 15%, 30% and 40% of slag replacing the cement content and having water to cement ratio of 0.3, 0.29, 0.28 and 0.27 by weight, respectively. The cement pastes were tested for compressive strength after water curing at 1, 3, 7 and 28 days. The various hydration products were identified using x-ray diffraction (XRD), differential thermal analysis (DTA) and scanning electron microscope (SEM) techniques. In the same context, the radiation attenuation coefficients expressed as linear attenuation coefficient, μ, of the investigated specimens were also determined after 28 days of hydration. The utilized radiation source comprised ^{137}Cs radioactive element with photon energy of 0.662 meV. In a similar manner, HVL and TVL for the tested samples were obtained. From the investigation, it has been revealed that the partial replacement of OPC on average 30% slag significantly increased compressive strength than the neat mixture at 28 days of curing. Although the enhancement of compressive strength upon replacing OPC with GGBFS, however the results of radiation parameters showed no significant effect of slag substitution on the attenuation of γ-rays.

Keywords: Blended cements · Linear attenuation coefficient · Half-value thickness · Tenth-value thickness

1 Introduction

Because of the wide application of nuclear science and technology in various fields as nuclear power plant, therefore, adequate and effective shielding is a prerequisite for the installation of such nuclear facilities to keep the radiation exposure below the dose limits recommended by the International Commission on Radiological Protection (ICRP). Shielding from gamma rays is more difficult than others because gamma photons have no mass and charge and hold high-energy, they can readily penetrate into the matter [1]. The photon interaction with the matter depends on its energy and the density of the shielding material [2]. The radiation shielding properties of a material are presented in terms of the linear attenuation coefficient (μ), which is defined as the

L. Struble and G. Tebaldi (eds.), *Materials for Sustainable Infrastructure*, Sustainable Civil Infrastructures, DOI 10.1007/978-3-319-61633-9_9

probability of a radiation interacting with a material per unit path length [3], and it is considered the most important quantity characterizing the penetration and diffusion of γ-rays in a medium. Its magnitude depends on the incident photon energy, the atomic number and the density (ρ) of the shielding materials [3]. Several works have been performed to obtain linear attenuation coefficients (l) theoretically and experimentally for different elements, compounds and mixtures [4], for different building materials [5], for concretes [6, 7] and for some aqueous solutions [8]. Concrete is a good radiation protector material because it has the characteristics which necessary to weaken the γ rays and neutrons [9]. The use of concrete for radiation shield is more focused on the nuclear requirements, not strength. Medium quality concrete is sufficient to achieve the strength of radiation shield, while the concrete of high- density can better resists the radiation. Quantity of material radiation includes: (1). Rate of exposure, which is defined as the ratio of number of photons after passing through thickness of protection material with the number of initial photons; (2). Coefficient of attenuation, which is a microscopic latitudes side, while the physical meaning of the latitudes sides (cross section) is the probability to absorb or scatter radiation. Gamma rays are attenuated in proportion to the atomic masses of the material. It is thus advantageous to make a gamma-ray shield of the densest material economically feasible [10]. In radiation shielding, absorbent material's properties must be well known. Shielding material must have high density, high radiation attenuation coefficient and structural properties like high strength.

Nuclear installations such as nuclear power reactors, particle accelerators, hot cells for radioisotopes production and radioactive waste conditioning facility, require shielding for radiation protection. This can be achieved by substituting concrete aggregates with some industrial by-products. Metallurgical slags which are produced as industrial by-products, if accumulated, are considered as hazardous waste materials from an environmental point of view. Most of these slags such as blast furnace slag, steel slag, copper slag and lead slag are used as aggregates in concrete components [11]. Mahdy et al. [12] used concretes containing magnetite as aggregate and mixed with three levels of silicafume to investigate the compressive strength and shielding properties. They concluded that magnetite as an aggregate and silica fume as a mineral admixture for concrete improve its compressive strength as well as its shielding properties. Portland cement is the main cementitious component of conventional concrete. The chemical composition of cement paste depends on the type of cement used in construction. Portland cement is the most commonly used cement for concrete shielding structures. Other cements with different chemical compositions are available but have not been used in construction of nuclear power plant concrete [9].

Many studies indicate that radiation affects the microstructure of cement paste. Lowinska-Kluge and Piszora [12] conducted a study on the microstructure of cement paste under various doses of gamma radiation using SEM. They concluded that pseudomorphoses had taken place after a dose of 130 MGy and that the microstructure of cement paste was changed significantly by the gamma radiation. Behaviors of cement paste and aggregate are known to differ under irradiation conditions: cement paste tends to contract slightly and aggregates tend to expand. Several researchers developed concrete properties to suit the shielding requirements. They mostly concentrate on

reducing the water contents or using other cementitious materials such as blast furnace slag, silica fume and polymeric compounds in addition to Portland cement [14, 15].

Ground granulated blast furnace (GGBFS) is a non-metallic material consisting essentially of silicates and alumino silicates of calcium [16]. It has been used as a supplementary cementitious material in Portland cement concrete, either as a mineral admixture or as a component of blended cement [17]. The partial replacement of ordinary Portland cement with GGBFS improves strength and durability of concrete by creating a denser matrix and thereby enhancing the service life of concrete structures. According to Hwang and Lin [18], GGBFS has the potential to replace cement in high percentages because of its in-built cementitious property.

In this study, the influences of replacing OPC with GGBFS on the mechanical properties of cement pastes were investigated. Also, the radiological properties of blended mixtures were studied by measuring the attenuation of γ- rays using radiation source comprised ^{137}Cs with photon energy of 0.662 meV. The obtained hydration products were identified using XRD, DTA and SEM techniques.

2 Experimental Details

2.1 Materials and Mix Proportions

Type I cement (42.5 N) with surface area of 2415 $cm^2\ kg^{-1}$ in compliance with the requirements of ASTM C150 [19], was used in the preparation of blended cements, obtained from Suez Cement Company, Egypt. GGBFS with surface area of 4000 $cm^2\ kg^{-1}$ was provided by Iron and Steel Company, Egypt. The chemical composition of ordinary Portland cement- OPC and GGBFS as conducted by XRF Spectrometer PW 1400 is presented in Table 1.

Table 1. Chemical composition of the starting materials

Oxides, %	OPC	GGBFS
SiO_2	21.26	37.81
Al_2O_3	4.49	13.14
Fe_2O_3	3.49	0.23
CaO	63.81	38.70
MgO	2.02	7.11
SO_3	3.11	1.19
Na_2O	0.14	1.03
K_2O	0.09	0.19
TiO_2	–	0.40
BaO	–	–
P_2O_5	–	0.17
L.O.I.	1.57	–
Total	99.98	99.97

For studying the effects of GGBFS as a supplementary cementing material on the properties of OPC either mechanical or radiological, five blended cement pastes designated as S0, S10, S15, S30 and S40 were prepared by the partial substitution of OPC with GGBFS at proportions of 0%, 10%, 15%, 30% and 40%. The w/b ratios for all mixtures were determined according to ASTM C187 [20] and had the values 0.3, 0.29 and 0.28 and 0.27 by weight, respectively. The details of mixture proportions are given in Table 2.

Table 2. Proportioning of blended cement mixtures, (%)

Mixture ID	OPC	GGBFS
S0	100	–
S10	90	10
S15	85	15
S30	70	30
S40	60	40

2.2 Specimen Preparation and Test Method

The dry mixtures were proportioned and mixed using a bench-mounted mixer of 5 L capacity to ensure complete homogeneity. Subsequently the required amount of mixing water was poured to the dry specimen. Continuous and vigorous mixing was conducted for 5 min. The specimens were cast in three layers into 25 × 25 × 25 mm cubic steel molds, then pressed until each layer being consolidated using a vibrating table. After the top layer was compacted, the surface of the paste was smoothed by the aid of thin edged trowel. After casting, the specimens were covered with wet burlap and polyethylene sheets, and then kept in the laboratory at room temperature for 24 h. After demolding, they were cured in tap water until the time of testing.

2.3 Compressive Strength Measurements

The hardened mixtures are subjected to the compressive strength test after 1, 3, 7 and 28 days of water curing according to ASTM C109 [21]. For stopping hydration process, crushed portions were stored in a solution of 1:1 methanol/acetone by volume for 24 h, then dried at 70 °C for 1 h and kept in an air-tight bottle.

2.4 X-ray Diffraction

The XRD analysis was carried out using a Philips PW 1050/70 Diffractometer. The data were identified according to the XRD software (pdf-2: database on CD-Release 2005). For conducting test, samples were passed through a 63 μm sieve.

2.5 Differential Thermal Analysis (DTA)

DTA was carried out by heating the sample in nitrogen atmosphere upto1000 °C with a heating rate of 20 °C/min using a DT-50 Thermal Analyzer (Schimadzu Co- Kyoto, Japan).

2.6 SEM Investigation

The microstructure of the hardened blended cement mortars was studied using SEM Inspect S (FEI Company, Holland) equipped with an energy dispersive X-ray analyzer (EDX). The data generated by EDX analysis consist of spectra showing peaks corresponding to the elements making up the true composition of the sample being analyzed. Elemental mapping of a sample and image analysis are also possible.

2.7 Gamma- Ray Attenuation Measurements

The linear attenuation coefficients of blended cements have been measured using the gamma spectrometer which contains sodium iodide NaI (Tl) scintillation detector [22]. The signals from detector were amplified and recorded by a Multi-Channel-Analyzer which communicates with Computer. The linear attenuation coefficients (μ) were determined by measuring the transmission of γ-rays through specimens of dimensions 10 × 10 × 10 cm and the γ-rays were obtained experimentally using ^{137}Cs radioactive elements with photon energies of 0.662 meV as standard sources with activities in micro curie (5 mCi). After 28 days of water curing, samples were taken out and left to oven dry at 105 °C with method used by Yilmaz et al. [23], subsequently each sample is arranged in front of a collimated beam obtained from gamma ray source for about 20 min. The linear attenuation coefficients (μ) were extracted from the mass attenuation coefficients (μ/ρ) calculated using a computer program named XCOM in a wide range of photon energies.

$$\mu = \left(\frac{1}{x}\right) \ln\left(\frac{N0}{N}\right) \tag{1}$$

Where N and N0 are the background subtracted number of counts recorded in detector with and without material between detector and source respectively and x is the material thickness (10 cm).

The half value layer (HVL) or the tenth value layer (TVL) of a material is used to describe the effectiveness of γ-ray shielding. Those can be calculated using equations below [24]:

$$\mathrm{HVL} = \frac{\ln 2}{\mu} \tag{2}$$

$$\mathrm{TVL} = \frac{\ln 10}{\mu} \tag{3}$$

3 Results and Discussion

3.1 Compressive Strength Development

The variation in compressive strength for all blended mixtures as a function of curing time at 1, 3, 7 and 28 days is graphically plotted in Fig. 1. The compressive strength increases with curing time for all blends, as a result of the continuous of hydration process with formation of hydration products that accumulates closing up some of available pore volumes giving more strength. The incorporation of high ratios of GGBFS in the cement pastes produces lower values of compressive strength at preliminary ages up to 7 days as compared to the neat OPC. This decrease can be caused by slower hydration reaction of slag than that of OPC, besides its latent hydraulic properties; however the compressive strength increases at later ages, due to the formation of extra amounts of crystalline calcium silicate hydrate (C-S-H) produced from the pozzolanic reaction between $Ca(OH)_2$ from OPC and amorphous SiO_2 of slag, that fills the large capillary voids in matrix, resulting in improved compressive strength [25]. This process of transformation is referred as "pore size refinement" [26]. The inclusion of 10% GGBFS (S10) in the blend matrix slightly enhanced 28- day compressive strength by nearly 0.7%, whereas the compressive strength has improved by about 3.5% at incorporation of 15% (S15). As it is also evident from the results that the partial replacement of OPC with 30% GGBFS (S30) significantly increased compressive strength by approximately 7.5%. The enhancement in compressive strength of the blended pastes is mainly attributed to the precipitation of additional amounts of

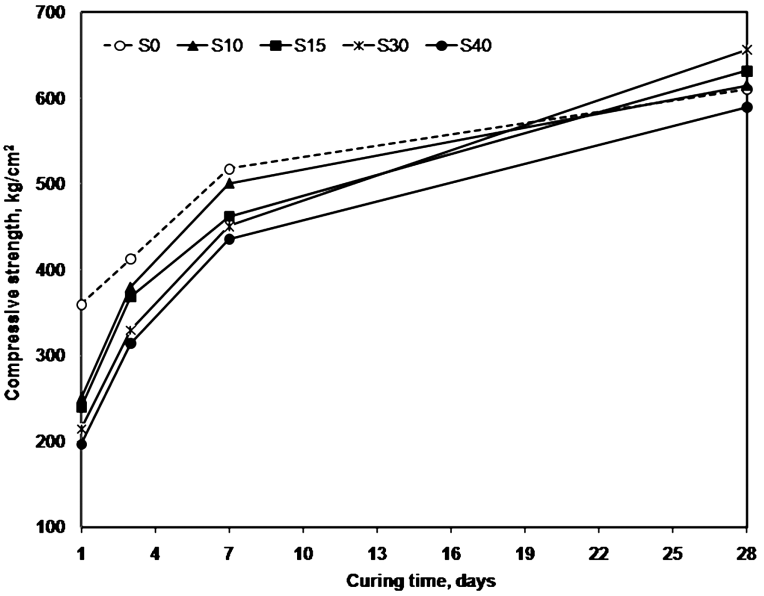

Fig. 1. Compressive strength development of cement pastes incorporating different ratios of ground granulated blast furnace slag after 28 days of water curing

secondary C-S-H gel and calcium aluminate hydrate (C-A-H) from the pozzolanic reaction in OPC-GGBFS system within the available pore volumes located in cement matrix. This gel is less dense and has more volume than primary C-S-H gel. Therefore it fills all the pores inside the cement matrix and makes it more impermeable with a consequent increase in compressive strength [26]. In contrast, the partial replacement of OPC with 40% GGBFS (S40) causes a marked decrease in the compressive strength values at all ages of hydration as compared to the neat OPC paste, as it had achieved a 45%, 24%, 13% and 3.5% lower compressive strength values at curing ages 1, 3, 7 and 28 days, respectively than the corresponding reference blend (S0). This decrease may be attributed to a reduction in OPC content that is responsible for the decrease in the amount of formed hydration products, mainly as C-S-H, which represents the main hydration product of the hardened cement pastes in addition to the dilution effect of OPC component with higher volumes of slag [27]. Finally, it can be concluded that the mixture incorporating 30% GGBFS as a partial replacement of OPC showed the highest compressive strength among all mixtures at curing age of 28 days, pointing out the effect of adding slag in enhancing the mechanical performance of cement pastes.

3.2 X-ray Diffraction (XRD)

The XRD patterns of cement mixtures incorporating 0%, 10%, 15%, 30% and 40% GGBFS and hydrated for 28 days in water are graphically represented in Fig. 2. Through the patterns, major peaks of portlandite (P) which are the expected product formed by OPC hydration along with calcium silicate hydrate (C-S-H), ettringite (E),

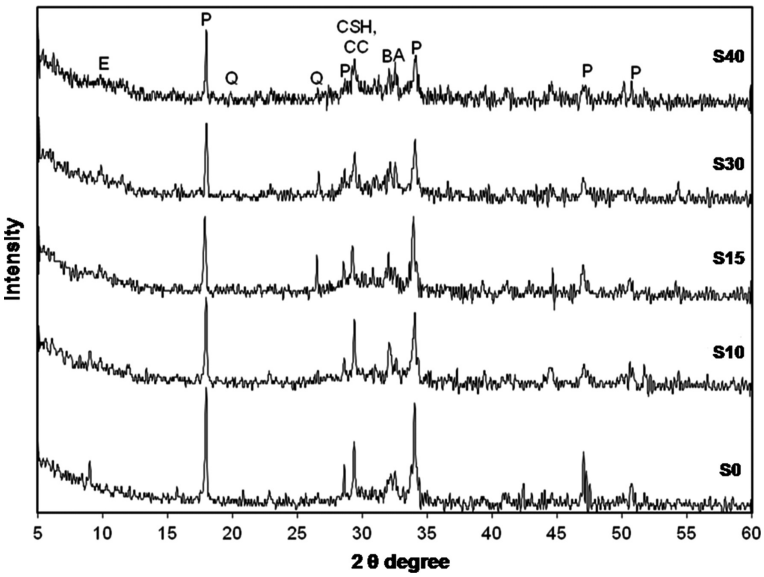

Fig. 2. X-ray diffraction patterns of cement pastes incorporating different ratios of ground granulated blast furnace slag after 28 days of water curing

calcium carbonate (CĆ), quartz (Q) as a main constituent of slag as well unhydrated cement phases (A is alite (C_3S), B is belite (β-C_2S) are detected. The patterns demonstrated that the intensity of the main peaks of portlandite located at 2θ of 17.97, 28.75 and 34.13 was diminished as GGBFS content increased, which in turn reflects the incidence of a pozzolanic reaction arising from the consumption of portlandite with the amorphous silicates of slag forming additional amounts of C-S-H phases. Obviously, ettringite phase was also observed in all blends and its intensity is sharply decreased with increasing GGBFS content, due to the consumption of free lime as well as the dilution of OPC by slag. On the other hand, peak intensity of C-S-H phase is decreased with the increase of slag than the neat mixture. Peaks of CĆ overlapped with C-S-H were also detected for all mixtures. Likewise, residual un- hydrated larnite-β-C_2S phases were also appeared even after 28 days of hydration; this is due to the rate of hydration of β-C_2S is slower than C_3S. In spite of the progress of hydration reaction, however the total amount of portlandite available for pozzolanic reaction has not yet been consumed, suggesting that the rate of consumption of free lime by blast furnace slag is too small at early ages, due to the latent hydraulic nature of slag material.

3.3 Differential Thermal Analysis (DTA)

Typical plots of DTA curves for cement pastes containing 0%, 10%, 15%, 30% and 40% GGBFS after curing in water for 28 days are given in Fig. 3. From the DTA thermograms, it was observed that five characteristic endothermic peaks located at 120, 187, 394, 480 and 715 °C are detected. The endotherms around 200 °C correspond to the decomposition of the nearly amorphous hydrates, mainly C-S-H as well as sulphoaluminate hydrates [28]. The temperature at which these compounds lose water depends upon the available $CaO:SiO_2$ ratio in the hydrated cement matrix. The decomposition of ettringite and/or monosulphate occurs at lower temperature and is

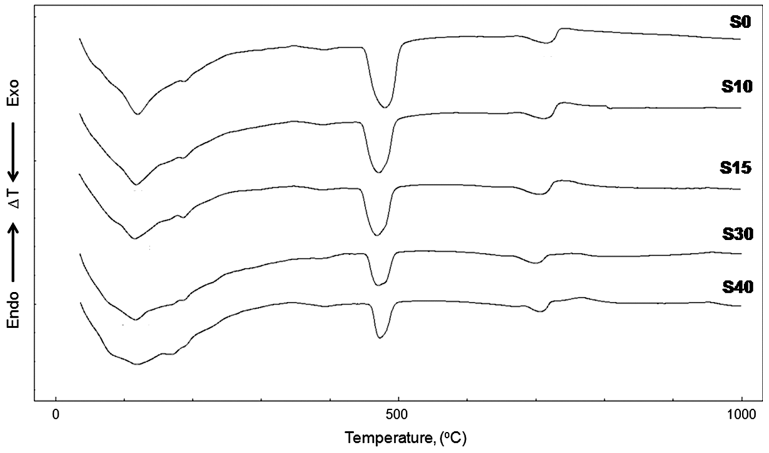

Fig. 3. DTA thermograms of cement pastes incorporating different ratios of ground granulated blast furnace slag after 28 days of water curing

overlapped by the C-S-H [29]. The peak area of C-S-H increases with GGBFS content up to 30%. Whilst, the endotherms observed around 394 °C may be denotes to the decomposition of hydrogarnet or be characterizing the decomposition of calcium aluminate silicate hydrate (CASH) and calcium aluminate hydrate (CAH) [30]. The sharp endotherms occurred around 480 °C indicates the dehydroxylation of portlandite-$Ca(OH)_2$ formed during OPC hydration [31]. It was observed that the intensity of portlandite peaks decreases sharply with increasing slag content. The reduction in [Ca $(OH)_2$] content indicates its consumption during pozzolanic reaction or may be the dilution of Portland cement by the slag. On the other hand, endotherms located around 715 °C represents the decarbonation of $CaCO_3$ and the intensity of peaks decrease with increase slag content in the blends.

3.4 Microstructural Analysis by SEM

Figure 4 showed the results of SEM analysis of the hardened cement pastes made of 0%, 15%, 30% and 40% GGBFS as a partial replacement of OPC after hydration in water for 28 days. The microstructure of the reference OPC paste as in Fig. 4a showed that the hydration products are formed and distributed all over the surface of the cement matrix. The hydration products existed mainly in the form of gel C-S-H(I) identified by its short needle-like form and some massive layers of $Ca(OH)_2$ identified by the fine-grained without crystal form distributed entirely in different regions of the cementitious matrix that have totally filled up capillary pore system in some areas, leaving others free of calcium hydroxide (CH). Likewise the micrographs indicated the presence of some voids permeate the microstructure. The partial replacement of OPC with 15% GGBFS accelerates the hydration phases (C_3S and C_2S) with sequential formation of massive hexagonal layers of calcium hydroxide and homogeneous well distributed foil-like C-S-H(II) phases that filled most of the available pore volume (Fig. 4b).

Also, as shown in Fig. 4b, the SEM micrographs appeared relatively dense and homogenous with close texture structure that has relatively high compressive strength than its original OPC micrographs after 28 days of curing. Further increasing GGBFS content in the matrix up to 30% (Fig. 4c) led to a relatively dense and compact microstructure in addition to more reduction in the un-hydrated GGBFS particles, indicating that most of the available hydrated lime from OPC is consumed by slag,s amorphous silica content to form additional amounts of secondary crystalline C-S-H phases that filled up the capillary pores inside the matrix, resulting in an extra enhancement in the specimen's morphology as compared to the microstructure of OPC paste (Fig. 4a) as well the reduction of CH may be due to the dilution of OPC by slag. On the opposite side, increasing the replacement of GGBFS up to 40% on the expense of OPC as described in Fig. 4d, led to a relatively permeable and less compact microstructure with pronounced formation of short fine-needle like ettringite, this hydration phase spread all over the surface of matrix, in addition to it filled the large pore voids. Finally, it can be concluded that high level replacement of GGBFS reduces the CH content librated from OPC hydration as a result of the dilution effect of OPC; which in turn resulted in the reduction of compressive strength of the blend at early ages than the corresponding S0 mix.

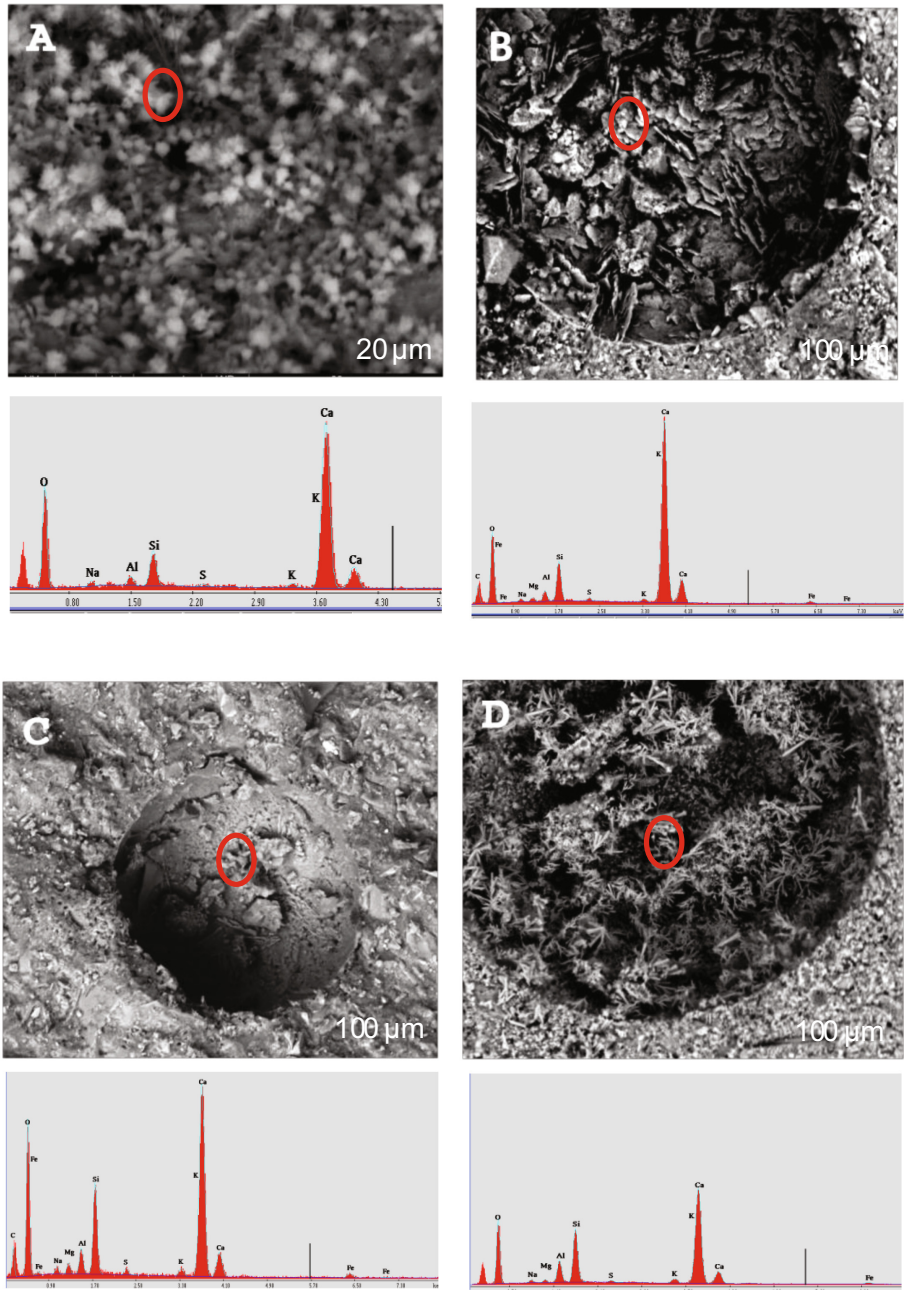

Fig. 4. SEM micrographs of cement pastes incorporating different ratios of ground granulated blast furnace slag after 28 days of water curing; (A) S0, (B) S15, (C) S30 and (D) S40

3.5 Gamma-ray Shielding Using ^{137}Cs Source

The values of measured of linear attenuation coefficient, μ, in the field of γ-rays emitted by ^{137}Cs at a given photon energy of 662 keV for the blended cements containing 0%, 15%, 30% and 40% GGBFS after hydration up to 28 days are graphically presented in Fig. 5. It has been reported that the linear attenuation coefficients decreased drastically with increasing concentration of GGBFS content in the blend. The reference mixture designated as S0 exhibited attenuation for gamma irradiation amounted to 0.294 cm^{-1}. As it is also evident from Fig. 5 the inclusion of 10% GGBFS reduced the linear attenuation by approximately 2%, whereas it decreased by an average of 3% at inclusion of 15%. As shown in Fig. 5, displayed that the higher the GGBFS content the lower the linear attenuation coefficient. The mixture containing 30% slag as a replacement showed lower value to the linear attenuation coefficient was estimated at 6% than the neat S0 paste. The same trend was observed for S40 when OPC was partially replaced with GGBFS up to 40%, since the linear attenuation coefficient of this mixture revealed approximately 8% times lower than the corresponding S0 paste. The decrease in linear attenuation coefficients for blended pastes may be associated with the dilution effect of OPC with high contents of GGBFS, besides the differences in specific gravities between OPC and GGBFS, where the latter presents lower specific gravity than OPC, which in turn affects the density of mixtures. The decrease in linear attenuation coefficient with the increase of slag content confirms a dependence on the material density and hence the provision of better shielding from γ-rays [32]. However, it can be seen from the results presented in Fig. 5 that partial replacement of GGBFS in cement pastes is not an option to be used for the purposes of gamma-radiation shielding.

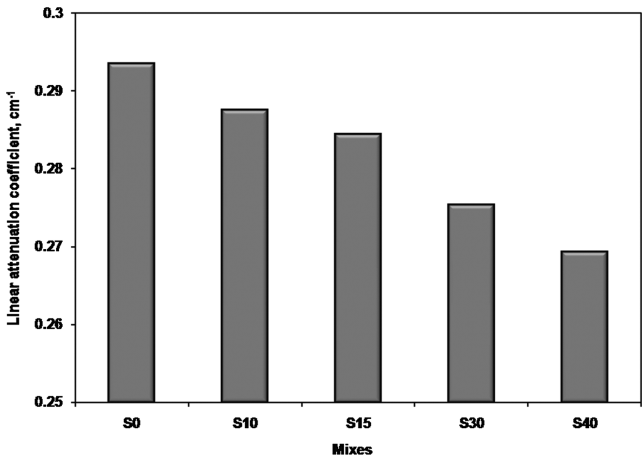

Fig. 5. The linear attenuation coefficients of cement pastes incorporating different ratios of ground granulated blast furnace slag after 28 days of water curing at photon energy of 662 keV for ^{137}Cs source

3.6 Half and Tenth Thicknesses (HVT & TVT)

Another parameter that is related to the linear attenuation coefficient, μ is called the half-value thickness, HVT, which is defined as the depth of shielding where the intensity of the primary photon beam is reduced by 50%. In similar fashion, the tenth-value thickness, TVT, is the depth required to reduce the photon intensity to one-tenth [33]. Half value thickness plays an important role on radiation shielding. The variations in HVT and TVT of blended cement pastes containing 0%, 15%, 30% and 40% GGBFS after hydration up to 28 days in the field of gamma rays at photon energy of 662 keV irradiated by ^{137}Cs are graphically represented in Figs. 6 and 7, respectively. Comparing Figs. 5, 6 and 7, it can be clearly noted that the HVT and TVT are inversely proportional to the linear attenuation coefficient values. Consequently, the values of both HVT and TVT are significantly increased with increasing of slag content up to 40%, where S40 mixture demonstrated the highest values relative to the S0 mixture that displayed the lowest values at the same dose of 662 keV. The HVT and TVT of the other blends (S10, S15 and S30) are gradually increased with increasing GGBFS content. The inclusion of 10% slag in the cement matrix enhanced the HVT and TVT on average 2% and the insertion of 15% enhanced them by approximately 3%. The same trend was observed for mixture S30, as it enhanced HVT and TVT by approximately 7% relative to the S0 paste. Figures 5 and 6 indicated also that the thickness increases as the density of pastes decreases, due to the dilution effect of the cementitious matrix by high volumes of slag. Finally, it can be said that blended cements with GGBFS had a negative effect on the attenuation of gamma-rays at photon energy dose of 662 keV, thus the slag-loaded cements would not be preferred as materials in building construction against γ- radiation.

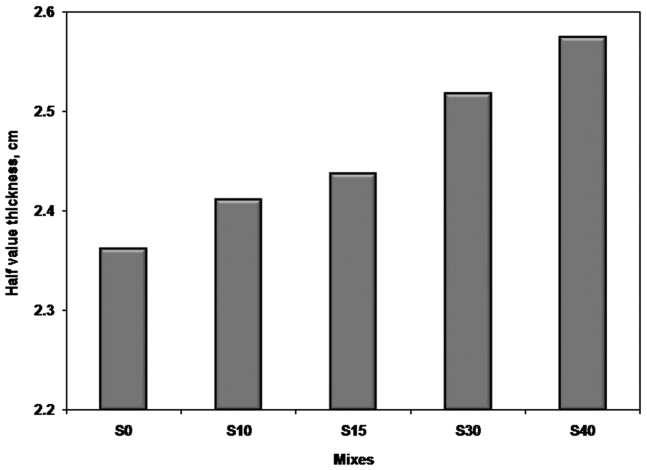

Fig. 6. Half-value thickness of cement pastes incorporating different ratios of ground granulated blast furnace slag after 28 days of water curing at photon energy of 662 keV for ^{137}Cs source

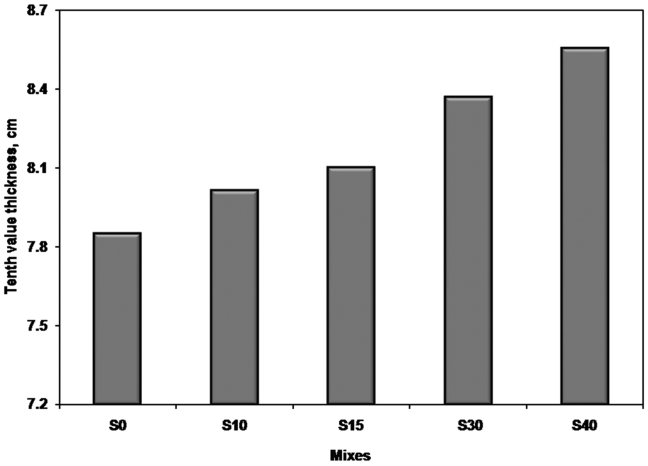

Fig. 7. Tenth-value thickness of cement pastes incorporating different ratios of ground granulated blast furnace slag after 28 days of water curing at photon energy of 662 keV for ^{137}Cs source

4 Conclusions

Based on the experimental results obtained from the undertaken study, the following conclusions can be summarized as follows:

1. The replacement of OPC with GGBFS in the preparation of blended cement led to an increase in the compressive strength after 28 days of water curing. The replacements at an average of 10%, 15% and 30% by weight enhanced it by approximately 0.7%, 3.5% and 7.5% folds, respectively comparing to the corresponding neat ordinary mixture of slag-free.
2. The inclusion of 40% GGBFS in the blend decreases the compressive strength at all hydration ages relative to the reference S0 paste. This tendency can be attributed to the hydraulic activity of the slag is less than of the OPC, Which had an impact in reducing the amount of hydration products, mainly as C-S-H, which represents the main binding centers of the hardened cement pastes.
3. From results it is clear that, with variation in slag content, there is no change in linear attenuation coefficients for all the studied mixtures at photon energy of 662 keV irradiated by ^{137}Cs source; meaning that slag has no obvious effect for enhancement of the shielding efficiency of cement against γ-rays in the thin thickness shield of 10 cm.
4. Whereas the attenuation of gamma rays depends primarily on the density of matter and as a result of the variation in specific gravities between OPC and GGBFS, it can be concluded that the slag-loaded cements are not suitable in building applications against γ- radiation.

References

1. Akkurt, I., Mavi, B., Akkurt, A., Basyigit, C., Kilincarslan, S., Yalim, H.: Study on Z-dependence of partial and total mass attenuation coefficients. J. Quant. Spectrosc. Radiat. Transf. **94**, 379–385 (2005)
2. Kallan, M.F.: Concrete Radiation Shielding. Longman Scientific and Technical, New York (1989)
3. Wood, J.: Computational Methods in Reactor Shielding. Pergamon Press, New York (1982)
4. Hubbell, J.H.: Photon mass attenuation and energy absorption coefficients from 1 keV to 20 MeV. Int. J. Appl. Radiat. Isot. **33**(11), 1269–1290 (1982)
5. Akkurt, I., Basyigit, C., Kilincarslan, S.: The photon attenuation coefficients of barite, Marble and limra. Ann. Nucl. Eng. **31**(5), 577–582 (2004)
6. Bashter, I.I.: Calculation of radiation attenuation coefficients for shielding concretes. Ann. Nucl. Eng. **24**(17), 1389–1401 (1997)
7. El-Sayed Abdo, A.: Calculation of the cross-sections for fast neutrons and gamma-rays in concrete shields. Ann. Nucl. Eng. **29**(16), 1977–1988 (2002)
8. Singh, K., Gagandeep, K., Sandhu, G.K., Lark, B.S.: Interaction of photons with some solutions. Rad. Phys. Chem. **61**(3–6), 537–540 (2001)
9. Mehta, P.K., Monteiro, P.J.M.: Concrete Microstructure, Properties and Materials, 2nd edn. Prentice Hall Inc., New Jersey (1993)
10. Walker, R.L., Grotenhuis, M.A.: Summary of shielding constants for concrete, ANL-6443 Reactor Technology (TID-4500. 16th (edn.) Amended), AEC Research and Development Report (1961)
11. Ermichev, S.G., Shapovalov, V.I., Sviridov, N.V., Orlov, V.K., Sergeev, V.M., Semyenov, A.G., Visik, A.M., Maslov, A.A., Demin, A.V., Petrov, D.D., Noskov, V.V., Sorokin, V.I., Uferov, O.I., Ornl, L.D., Ridge, O.: High-density concrete with ceramic aggregate based on depleted uranium dioxide, IHLRWM, Las Vegas, NV, 30 April–4 May, pp. 880–884 (2006)
12. Mahdy, M., Speare, P.R.S., Abdel-Reheem, A.H.: Shielding properties of heavyweight, high strength concrete. In: 2nd Material Specialty Conference of the Canadian Society for Civil Engineering, 5–8 June (2002)
13. Kluge, A.L., Piszora, P.: Effect of gamma irradiation on cement composites observed with XRD and SEM methods in the range of radiation Dose 0–1409 MGy. Acta Phys. Pol., A **114**(2), 399–411 (2008)
14. Gencel, O., Brostow, W., Ozel, C., Filiz, M.: Concretes containing hematite for use as shielding barriers. Mater. Sci. **16**(3), 249–256 (2010)
15. Gencel, O., Brostow, W., Ozel, C., Filiz, M.: An investigation on the concrete properties containing colemanite. Int. J. Phys. Sci. **5**(3), 216–225 (2010)
16. Siliceous by-products for use in concrete, Final Report, RILEM Technical Reports 73-SBC RILEM Committee, 21(1), pp. 69–80 (1988)
17. Shi, C., Qian, J.: High performance cementing materials from industrial slags—a review. Resour. Conserv. Recycl. **29**(3), 195–207 (2000)
18. Hwang, C.L., Lin, C.Y.: Strength development of blended blast furnace slag cement mortars. In: Malhotra, V.M. (ed.) Proceedings of the 2nd International Conference on Fly Ash, Silica Fume, Slag and Natural Pozzolana in Concrete, SP-91, pp. 1323–1340. American Concrete Institute, Farmington Hills, Mich (1986)
19. ASTM C150, Standard Specification for Portland Cement (2015)
20. ASTM C187, Standard Test Method for Amount of Water Required for Normal Consistency of Hydraulic Cement Paste (2011)

21. ASTM C109, Standard Test Method for Compressive Strength of Hydraulic Cement Mortars (Using 2-in. or [50-mm] Cube Specimens) (2013)
22. Akkurt, I.: Effective atomic and electron numbers of some steels at different energies. Ann. Nucl. Eng. **36**(11–12), 1702–1705 (2009)
23. Yilmaz, E., Baltas, H., Kiris, E., Ustabas, I., Cevik, U., El-Khayatt, A.M.: Gamma ray and neutron shielding properties of some concrete materials. Ann. Nucl. Eng. **38**(10), 2204–2212 (2011)
24. Akkurt, I., Akyildirim, H., Mavi, B., Kilincarslan, S., Basyigit, C.: Gamma-ray shielding properties of concrete including barite at different energies. Prog. Nucl. Eng. **52**(7), 620–623 (2010)
25. Islam, M.M., Islam, M.S., Mondal, B.C., Islam, M.R.: Strength behavior of concrete using slag with cement in sea water environment. J. Civ. Eng. (IEB) **38**(2), 129–140 (2010)
26. Bakker, R.F.M.: Permeability of blended cement concretes. In: Proceedings of the First CANMET/ACI International Conference on Fly Ash, Silica Fume, Slag and other Min eralby-Products in Concrete-SP-79, ACI, Detroit., pp. 589–606 (1983)
27. Amin, M.S., El-Gamal, S.M.A., Abo-El-Enein, S.A., El-Hosiny, F.I., Ramadan, M.: Physico-chemical characteristics of blended cement pastes containing electric arc furnace slag with and without silica fume. J. HBRC **11**(3), 321–327 (2015)
28. Lea, F.M.: The Chemistry of Cement and Concrete, 4th edn, p. 184. Edward Arnold, London (1974)
29. Heikal, M., Helmy, I., El-Didamony, H., Abd El-Raoof, F.: Electrical properties, physico-chemical and mechanical characteristics of fly ash-limestone-filled pozzolanic cement. Ceram. Silik. **48**(2), 49–58 (2004)
30. Ubbriaco, P., Calabrese, D.: Solidification and stabilization of cement paste containing fly ash from municipal waste. Thermochim. Acta **321**(1–2), 143–150 (1998)
31. Singh, S.P.: Use of thermo analytical techniques in the study of hydration of cement. In: Proceedings of the National Conference on Thermal Analysis, 1, BARC, Mumbai, 69 (2002)
32. Akkurt, I., Akyıldırım, H., Mavi, B., Kilincarslan, S., Basyigit, C.: Radiation shielding of concrete containing zeolite. Radiat. Meas. **45**, 827–830 (2010)
33. El- Dakroury, A., Gasser, M.S.: Effects of SF and Ilmenite on the Chemical. Mech. Radiat. Behav. Matrices Used Solidification Wastes, Nature Sci. **10**(5), 92–99 (2010)